Received: 30 November 2021 | Accepted: 1 June 2022

DOI: 10.1002/aps3.11502

APPLICATION ARTICLE

Applications in Plant Sciences

# A low-cost high-throughput phenotyping system for automatically quantifying foliar area and greenness

**Tyler Thrash**[1,2] | **Hansol Lee**[1,3] | **Robert L. Baker**[1,4]

[1]Department of Biology, Miami University, 212 Pearson Hall, Oxford, Ohio 45056, USA

[2]Graduate Program in Biology, Saint Louis University, 301 Macelwane Hall, St. Louis, Missouri 63103, USA

[3]Graduate Program in Ecology, Evolution, and Environmental Biology, Miami University, 212 Pearson Hall, Oxford, Ohio 45056, USA

[4]Inventory and Monitoring Division, National Park Service, 1201 Oakridge Drive, Suite 150, Fort Collins, Colorado 80525, USA

**Correspondence**

Tyler Thrash, Graduate Program in Biology, Saint Louis University, 301 Macelwane Hall, St. Louis, Missouri 63103, USA.
Email: tyler.thrash@slu.edu

## Abstract

**Premise:** With modern advances in genetic sequencing technology, plant phenotyping has become a substantial bottleneck in crop improvement programs. Traditionally, researchers have manually measured phenotypic traits to help determine genotype–phenotype relationships, but manual measurements can be time consuming and expensive. Recently, automated phenotyping systems have increased the spatial and temporal density of measurements, but most of these systems are extremely expensive and require specialized expertise. In the present paper, we develop and validate a low-cost, scalable, high-throughput phenotyping (HTP) system for automating the measurement of foliar area and greenness.

**Methods:** During a greenhouse experiment on the effects of abiotic stress on *Brassica rapa*, we collected images of hundreds of plants every hour for over a month with a system that cost approximately US$1000.

**Results:** In comparison with manually acquired images, this HTP system was able to produce similar estimates of foliar area and greenness, developmental trends, and treatment effects. Foliar area was correlated between the two image sets, but greenness was not.

**Discussion:** These findings highlight the potential of HTP systems built from low-cost hardware and freely available software. Future work can use this system to investigate genotype–environment interactions and the genetic loci underlying morphological changes resulting from abiotic stress.

KEYWORDS

agriculture technology, controlled environment, image analysis

The ongoing worldwide food crisis emphasizes the need for reducing the cost of agricultural production (Von Braun, 2008; Ray et al., 2013; Challinor et al., 2014). Investing time and money into research on genotype–phenotype relationships for crops can improve agricultural productivity in the long term (Von Braun, 2008; Challinor et al., 2014). While high-throughput genomics has rapidly become cost- and time-efficient, the throughput and cost of phenotyping has become a major limitation in most crop improvement programs (Casto et al., 2021). Traditionally, phenotyping has involved manual measurements of plant organs and yield. While manual measurements may benefit from the expertise of the experimenter, manual measurements by novices can also be useful given supportive devices or computer interfaces (Giuffrida et al., 2018).

Recent advances in hardware and software have allowed the development of high-throughput phenotyping (HTP) systems for automatically measuring plant traits at higher spatial and temporal densities (for a review, see Yang et al., 2020). The more advanced systems consist of several different imaging stations for non-invasive measurements, computer-controlled conveyors for moving plant pots to different stations, and automated plant care (Yang et al., 2020; Casto et al., 2021). While these systems can provide a wealth of data on a variety of phenotypes, they are often costly to install and operate. To help address the

worldwide food crisis, the cost and throughput of HTP systems need to be improved (Prasanna et al., 2013; Casto et al., 2021). Toward this end, the present study demonstrates and validates the use of a low-cost HTP system for automatically quantifying foliar area and greenness.

The cost of HTP systems for crop improvement is often driven by the automation of movement and plant care, the temporal density of the measurements required to detect a particular developmental pattern, and specialized hardware for acquiring physiological and/or hyperspectral data (Yang et al., 2020). The movement of plants toward sensors reduces the number of sensors that need to be integrated into the system. The automation of plant care also helps standardize the environment in which plants are grown (Brien et al., 2013). Compared to measurements by human observers, automated measurements can be more precise, provide spatially dense data to be archived for additional analyses, and increase the temporal density with which measurements can be taken. The temporal density of measurements is an especially important consideration for the study of phenotypic changes during plant development (Berger et al., 2012; Ge et al., 2016).

Hyperspectral data (e.g., the amount of light reflected at wavelengths beyond the visible spectrum) may be especially useful for inferring physiological traits such as leaf water content (Ge et al., 2016), but specialized hardware is required for data acquisition (for a review, see Li et al., 2014). Hyperspectral cameras are also more expensive than the standard digital cameras that produce RGB images. The need for such expensive hardware limits the temporal density of measurements by requiring plants to be moved toward the sensors (Casto et al., 2021). In addition, hyperspectral data require more time to acquire and more storage space to maintain. Compared to hyperspectral images, RGB images may also be more useful for extracting phenotypes from heterogeneous canopies in the field because of the effects of leaf overlap on near-infrared reflectance (Kefauver et al., 2015). Consequently, RGB cameras may be employed in both agricultural settings with large plots of crops and greenhouse settings with smaller plots that systematically vary with respect to treatment. Similar analyses based on RGB images can also be used for more precise measurements of individual plants. Indeed, for a variety of settings, HTP systems with a larger number of relatively cheap sensors (e.g., RGB cameras) may improve the temporal density of measurements and scalability without necessarily sacrificing data quality.

While RGB images for extracting morphological traits are relatively easy and cheap to acquire, there are several different indices that can be used to compute greenness and extract plants/organs from these images. The simplest greenness index is when the intensity of a pixel along the G dimension is above a particular threshold (e.g., Kefauver et al., 2015). The main challenges with this simple greenness index are that it includes a wide range of wavelengths and that it often does not produce enough contrast between the plant/organ of interest and the background. To address the former challenge, "greener area" has been defined as the intensity of a pixel at a narrower set of wavelengths, thereby excluding less healthy plants that may have become more yellow (e.g., Kefauver et al., 2015). Similarly, Humplík et al. (2015) converted RGB values to a hue-saturation-value (HSV) color space and defined a greenness index as within a particular range of H values. Depending on the range selected for H values, this HSV-based index may be more similar to either the simple greenness index or the greener area defined above. In addition, Awlia et al. (2016) divided hues into several different greenness categories based on RGB values and assessed treatment effects separately for each category.

To produce more contrast between plants and the background of RGB images, several different indices have been defined as the difference or ratio of pixel values along multiple spectra. For example, An et al. (2016) defined a normalized green-red difference index as the difference between the G and R values of a pixel divided by the sum of G and R values for that pixel. Ge et al. (2016) incorporated the B value into their greenness index, defined as twice the G value divided by the sum of the B and R values for a pixel. Similarly, Richardson et al. (2007) measured canopy cover at the landscape scale using a greenness index defined as twice the G value minus the B and R values. Although the incorporation of the B value may improve the contrast between plants and background for landscape scenarios with the sky as the background, these indices have not yet been systematically compared. In addition, many studies have employed machine learning for separating plants from their background without an explicitly defined greenness index (e.g., Minervini et al., 2017). Regardless of the specific approach, the ability to clearly separate plants from their background and quantify useful traits using RGB images would allow HTP systems to include additional sensors at a relatively low cost while maintaining or even improving the temporal density of measurements.

The present study demonstrates and validates the use of a low-cost and scalable HTP system that allows for higher temporal density of measurements and can be employed in a large variety of agricultural and experimental settings. The primary goal of this study is to demonstrate that such a system, developed with limited resources, can accurately and automatically measure useful plant traits in a scalable manner. The HTP system described here consists of eight consumer-grade digital cameras that were installed above benches of greenhouse plants and controlled wirelessly with a Raspberry Pi computer. For validation, we deployed this system during an experiment on salt stress for two genotypes of *Brassica rapa* L. During this experiment, the system acquired nearly 6000 RGB images of greenhouse benches containing up to 70 plants each. We also manually acquired high-resolution RGB images of each individual plant at five different time points during the experiment for comparison with the images acquired by the HTP system.

# METHODS

## Experimental design

Initially, we planted 280 pots of *B. rapa*, each pot containing three seeds of either L58 or R500 genotypes. To maintain the integrity of the different genotypes, seeds were manually separated from chaff. L58 is a leafy vegetable variety of *B. rapa* similar to Chinese cabbage or pak choi (Toxopeus et al., 1987). R500 is a yellow sarson oil seed variety of *B. rapa* that tends to grow taller and allocate more resources toward seed production (Baker et al., 2019). Plants were thinned to only the single healthiest plant per pot shortly after germination.

The plants were grown on four benches in a greenhouse (Miami University, Oxford, Ohio, USA; 39°30′11.7″N 84°42′0″W) with Pro 325e LED lamps (Lumigrow, Emeryville, California, USA) that extended the daylength to a consistent 16 h. Each bench contained HOBO MX2202 sensors (ONSET, Bourne, Massachusetts, USA) to measure temperature throughout the experiment. Three smartPAR light sensors (Lumigrow) were spaced throughout the greenhouse and above supplemental LED lights to log the solar daily light integral (DLI). Each bench also contained an equal number of pots for each of the two genotypes for several different substrates and pot sizes. The pots were either 5.08 cm × 5.08 cm × 8.89 cm or 7.62 cm × 7.62 cm × 8.89 cm and contained either a 1:2 kg mix of M2 Professional Mix potting soil (BFG Supply, Burton, Ohio, USA) and commercial-grade fine sand (Quickrete, Atlanta, Georgia, USA) with a slow-release 18-6-12 Osmocote fertilizer (ICL Specialty Fertilizers, Summerville, South Carolina, USA), a similar potting soil/sand mix without fertilizer, or a triple-rinsed calcined non-swelling illite clay medium (Turface MVP, PROFILE products, Buffalo Grove, Illinois, USA) with fertilizer. The purpose of testing these different substrates was to determine whether water with or without salt would readily flow through the media and keep the salt concentration of the soil constant. All of the pots were composed of highly reflective black plastic and were randomly arranged on black plastic trays containing the same pot sizes and substrates.

Immediately before planting, the media in each pot was saturated with either tap water (control condition) or 0.3% (54.34 mM) NaCl (Fisher Scientific, Waltham, Massachusetts, USA) water (salt condition) until the water had soaked the media and began emerging from the bottom of the trays (i.e., "flow-through" method; Hasanuzzaman et al., 2018). All pots continued to be watered with either tap or salt water to field capacity throughout the experiment.

Two types of images were acquired during the experiment. First, we collected images of whole benches using the HTP camera system (i.e., with eight different cameras) every hour throughout the experiment. A scale diagram of each bench, with two lights and two GoPro cameras, is provided in Figure 1. Second, we collected high-resolution images of each individual plant at five different time points after thinning but before the plants had bolted and flowered. These high-resolution images were acquired under controlled lighting conditions with a Canon DSLR camera (Canon, Tokyo, Japan) with a fixed-length lens.

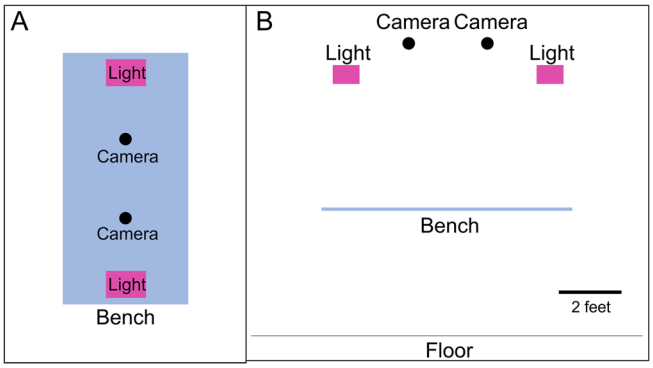


**FIGURE 1** A scale diagram of each bench with two lights and two GoPro cameras. (A) Overhead view. (B) Side view.

## Camera system

The main components of the system were eight GoPro Hero3 cameras (http://www.gopro.com; GoPro Inc., San Mateo, California, USA) and a Raspberry Pi 3B+ computer (https://www.raspberrypi.org; Raspberry Pi Foundation, Cambridge, United Kingdom). The GoPros were placed so that each camera could capture an image from a similar perspective approximately 1.6 m above a bench in the greenhouse every hour for over a month (i.e., during the course of a long experiment). Two GoPros were placed above each of four benches, approximately 0.3 m apart. The images acquired by each pair of GoPros overlapped to provide some redundancy in the measurement of each plant. During the experiment, the Pi computer communicated with the cameras wirelessly from a different room. This prevented the relatively fragile Pi computer from being damaged by the sun and/or humidity in the greenhouse.

This model of Pi computer had a 64-bit quad-core processor running at 1.4 GHz with 1 GB of RAM and a dual-band (2.4 and 5 GHz) wireless local area network (LAN). The Pi also contained a 16 GB microSD card that was pre-loaded with several different types of software, including NOOBS (for installing the Raspbian operating system), Chromium (an internet browser for Linux systems), Raspbian terminal, and a file manager (similar to Windows Explorer). The Pi hardware also included an HDMI port, four USB ports, and a microSD card reader.

The GoPro cameras were equipped with wireless networks using the GoPro application for Android. Although this wireless capability is primarily intended to be used with either a GoPro remote or the GoPro phone application, in principle the GoPros can be connected to (and manipulated by) any modern computer. Each GoPro was also equipped with a 128 GB microSD card in

order to prevent storage problems over the course of a long experiment. The cost of the system was approximately US $1000. This cost estimate includes one Raspberry Pi computer (US$35), eight GoPro Hero3 cameras (US$92 each), and eight 128 GB microSD cards (US$29 each).

All of the commands for connecting to each camera's wireless network, capturing images on the cameras, and copying images were executed as shell scripts in the Raspbian terminal application. To automatically schedule tasks for the camera system, the desired time to execute each shell script was entered as a crontab. A crontab is a regular schedule for Linux systems to automatically execute particular functions.

Creating the shell scripts for connecting to each GoPro's wireless network (and switching between them) required a few additional steps. First, the GoPro's wireless network had to be set up manually on the GoPro by defining the wireless network name and password using the GoPro application for Android. Only once during setup, the Pi had to be manually connected to the wireless network of each GoPro. Once the Pi was connected to one of the wireless networks, the key needed to automatically connect to this network was available in an automatically generated configuration file. The service set identifier (SSID) and pre-shared key (PSK) from this wireless network were then copied into another text file. Once the key information was saved for each GoPro's wireless network, another shell script was created to connect to or switch between them. An additional shell script was written to turn on the GoPro (assuming the corresponding wireless network was already connected) and take a picture.

Image acquisition began immediately after plant thinning. During the experiment, the Pi computer took a picture from each of the eight GoPros once every hour. Only images taken during the day without supplemental lighting were used for the analyses. Each of these pictures was initially stored on the microSD cards of the GoPros themselves, but at night, these pictures could be automatically and wirelessly copied to an external hard drive that was mounted to the Pi computer and remotely accessible. This approach allows researchers to check on the system and, if desired, analyze the data every night throughout the experiment for near real-time results without interfering with the system's functioning.

## Image processing and analyses

For images representing different steps in the image analyses, see Figures 2 and 3. Several Python libraries were needed in order to read raw image files (*rawpy* version 0.15.0, https://pypi.org/project/rawpy/0.15.0/), convert between file formats (*imagio* version 2.9.0, https://imageio.readthedocs.io/en/stable/; *numpy* version 1.18.2, https://numpy.org/doc/1.18/; *PIL* version 1.1.7, https://pypi.org/project/Pillow/1.0/), read date and time data from the HTP images (*exifread* version 2.1.2, https://pypi.org/project/ExifRead/2.1.2/), read csv files listing experimental conditions (*csv* version 3.7, https://docs.python.org/3.7/library/csv.html), and extract and specify file paths (*pathlib* version 3.7, https://docs.python.org/3.7/library/pathlib.html). Initially, both image types (GoPro and DSLR) were automatically cropped to remove extra space

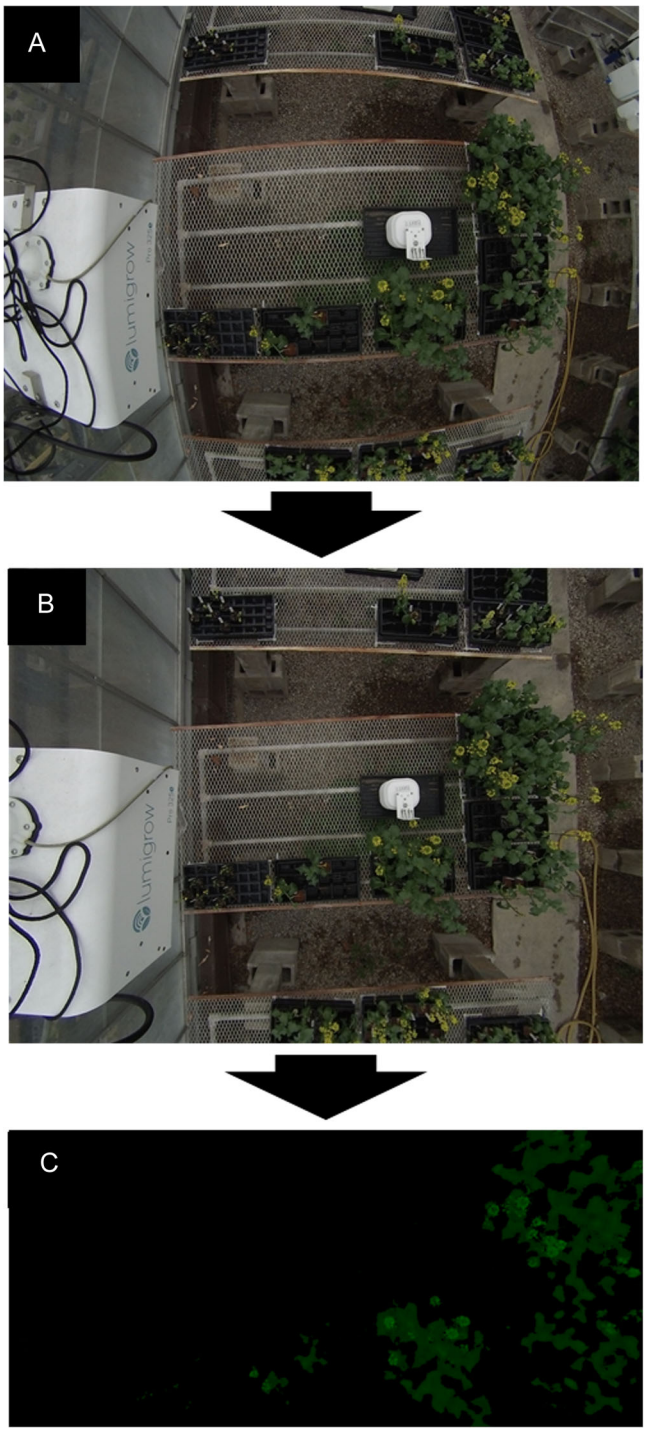


**FIGURE 2** Examples representing different steps of the bench-level image analyses. (A) One of the original images acquired using one of the GoPro cameras toward the end of the experiment. (B) The same image after correcting for the distortion caused by the camera's fisheye lens. (C) An image representing the greenness index for each pixel of the camera image after automatically cropping around the bench.

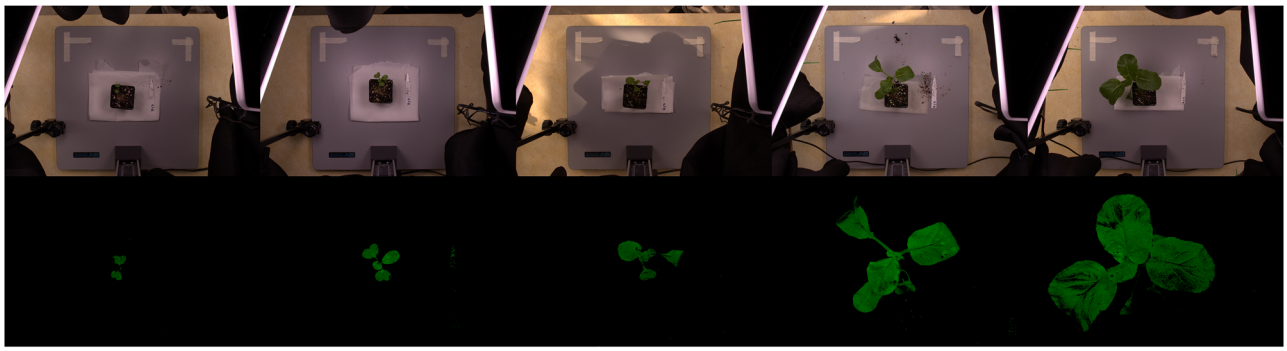

**FIGURE 3** Examples of DSLR images that were manually acquired for the same plant on different days throughout the experiment (top) and images representing the greenness index for each pixel of the DSLR image after cropping around the platform (bottom).

around the bench/platform that did not contain plants. To reduce the manual steps required for analysis, images from all eight GoPro cameras were cropped using the same parameters, despite occupying slightly different positions above the different benches. For each image, we then automatically corrected for any distortion caused by the camera's fisheye lens using the *lensfunpy* (version 1.8.0, https://pypi.org/project/lensfunpy/1.8.0/) and cv2 (https://pypi.org/project/opencv-python/) libraries for Python. The greenness index (2*G – R – B) was then calculated for each pixel of each corrected RGB image. Pixels with extremely high values (above 202) were removed because they most often represented the highly reflective black plastic. Pixels with extremely low values (below 29) were also removed because they most often represented small non-plant artifacts. To calculate mean foliar area per bench, the number of remaining "green" pixels were counted for each bench-level image and then divided by the number of plants on that bench. Mean foliar area was determined for the DSLR images by counting the number of green pixels for each individual plant image and then averaging over the number of individual plants on each bench. The mean greenness of each image was then calculated as the mean greenness index over pixels with values above zero.

All of the inferential statistics for correlational and linear mixed effects modeling was conducted in RStudio 1.3.1073 with the *lme4* (version 1.1-23), *lmerTest* (version 3.1-2), and *ggplot2* (version 3.3.5) libraries.

## RESULTS

Developmental trends for foliar area are shown in Figures 4 and 5. Increases in foliar area during plant development are visible and similar in scale for the HTP and DSLR images. This growth is also substantially greater for control plants compared to plants grown under salt conditions for both HTP and DSLR images. Developmental trends for greenness are shown in Figures 6 and 7. The control and salt condition plants do not appear to differ in development in terms of greenness given the possible range of greenness values. Although previous research has found that salt stress can reduce chlorophyll content in *Solanum nigrum* L. (Abdallah et al., 2016), researchers have had difficulty detecting significant differences in greenness indices for other species (e.g., *Arabidopsis thaliana* (L.) Heynh.; Awlia et al., 2016). Notably, our HTP system derives similar growth patterns and treatment effects as the manually acquired DSLR images but at a much higher temporal density.

We also computed correlations between the HTP and DSLR data sets in terms of both mean foliar size and mean greenness separately for plants grown under control and salt conditions. The correlated data include only days in which both HTP and DSLR images were acquired. In terms of foliar size, HTP and DSLR data were significantly correlated for both control ($r(3) = 0.996$, $P < 0.001$) and salt ($r(3) = 0.987$, $P = 0.002$) conditions. In terms of greenness, HTP and DSLR data were not significantly correlated for either control ($r(3) = -0.0002$, $P = 0.9997$) or salt ($r(3) = -0.266$, $P = 0.665$) conditions.

Linear mixed models were used to assess the fixed effects of and interactions between treatment (salt versus control) and calendar days since germination on mean foliar area ($cm^2$) and greenness (separately) for HTP and DSLR images (separately). Bench number was included as a random effect for all four models, and solar DLI was averaged over the three sensors and included as an additive covariate for the two models with the HTP data. Across calendar days, the mean solar DLI ranged from 1.19 to 13.97 with a mean of 8.05 and a standard deviation of 3.62. The exact models for these analyses in R notation are available in Appendix S1.

The fixed effects and covariates for each model of the bench-level analyses are summarized in Table 1. To summarize the bench-level analyses, we found significant fixed effects of days after germination and two-way interactions between treatment and days after germination in terms of (mean) foliar area for both the HTP and DSLR images. This analysis also revealed a fixed effect of solar DLI on mean foliar area for the HTP images and a fixed effect of treatment on foliar area for the DSLR images. For the HTP images, we also found a fixed effect

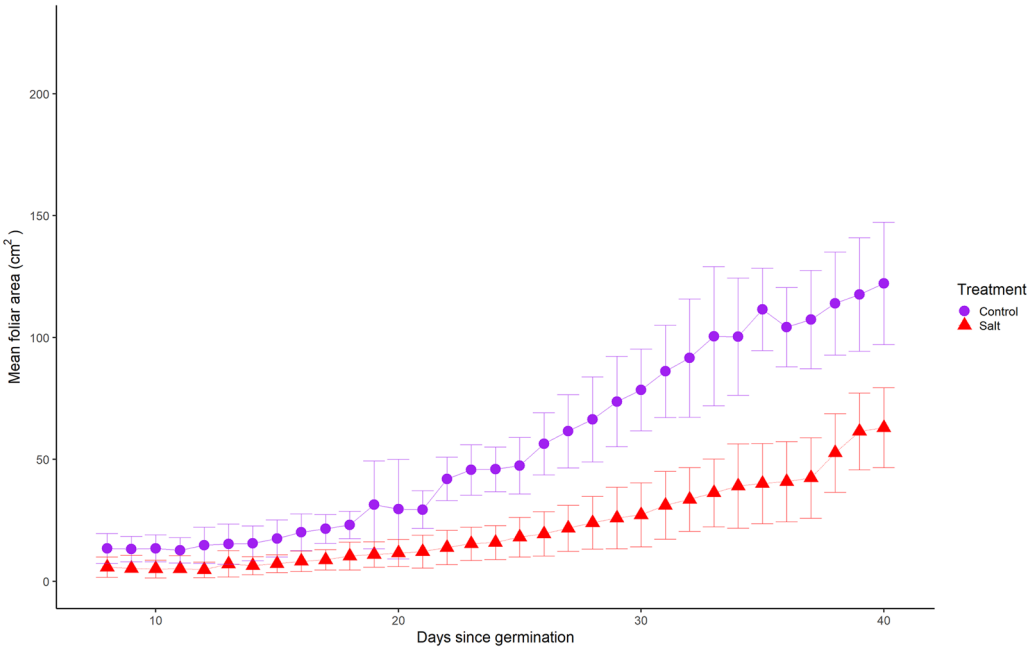


**FIGURE 4** A graph depicting differences between control and salt treatments in terms of foliar area (cm$^2$) for the HTP images and how these differences increase over days since germination. Each data point represents the mean of 23 to 36 measurements (five to nine measurements per camera per bench). Error bars represent the standard deviation of foliar area estimates across images from the same day.

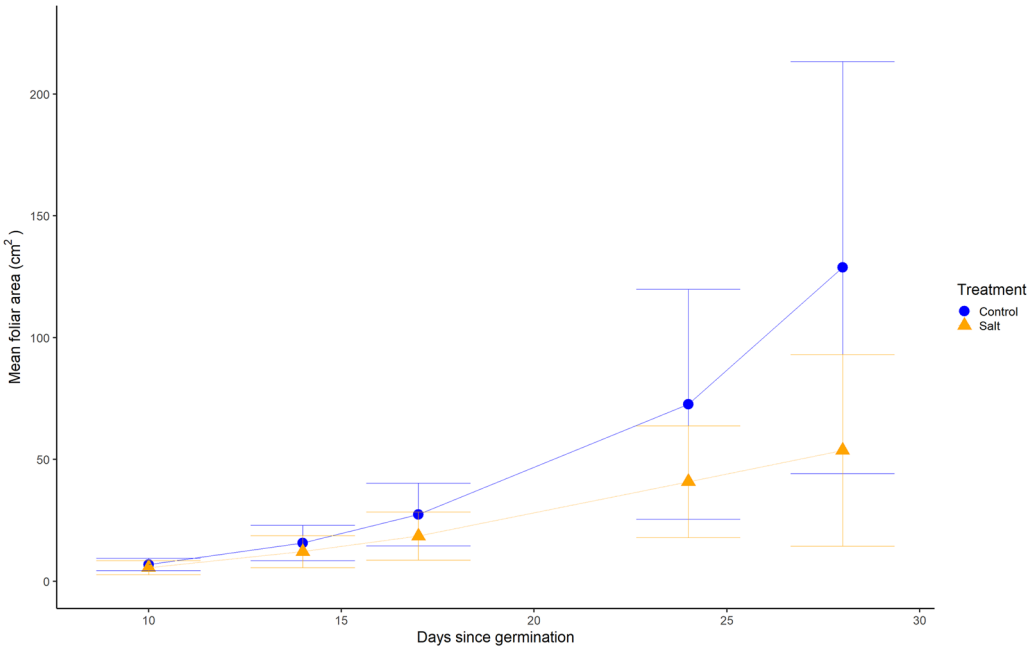


**FIGURE 5** A graph depicting differences between control and salt treatments in terms of foliar area (cm$^2$) for the DSLR images and how these differences increase over days since germination. Each data point represents the mean of between 102 and 141 measurements. Error bars represent the standard deviation of foliar area estimates across images from the same day.

of days after germination, a fixed effect of solar DLI, and an interaction between treatment and days after germination in terms of greenness. However, for the DSLR images, we only found a fixed effect of days after germination on greenness.

## DISCUSSION

The present paper describes the development and validation of a low-cost, automated, and scalable HTP system for measuring foliar area and greenness. In comparison with

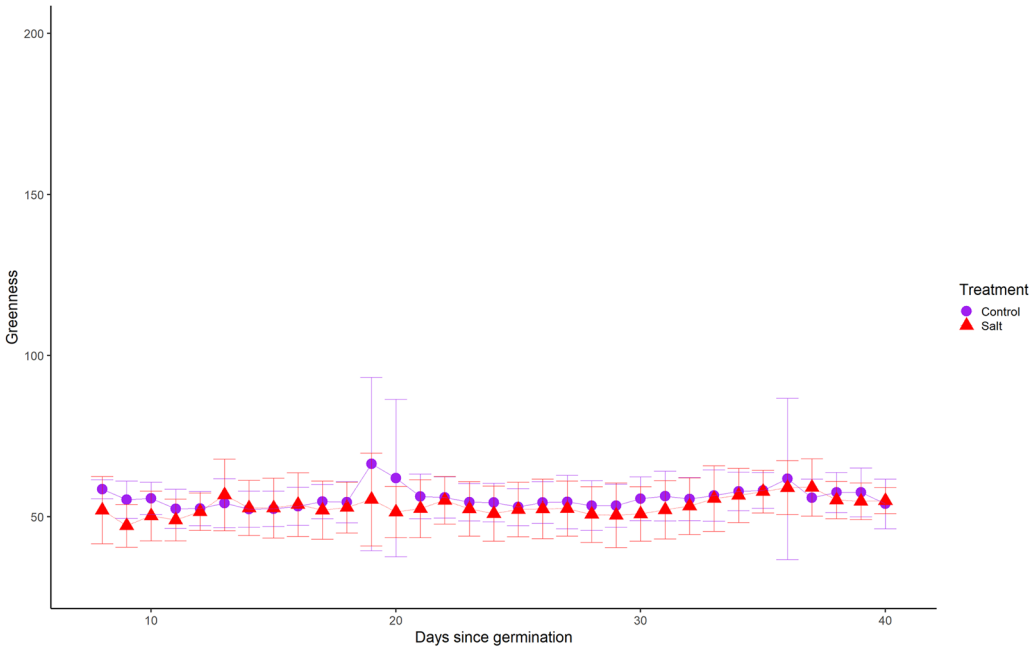


**FIGURE 6** A graph depicting changes in greenness as a function of days since germination for the HTP images after control and salt treatments. Here, the *y*-axis is truncated to represent the range of possible greenness values after image processing. Each data point represents the mean of 23 to 36 measurements (five to nine measurements per camera per bench). Error bars represent the standard deviation of greenness estimates across images from the same day.

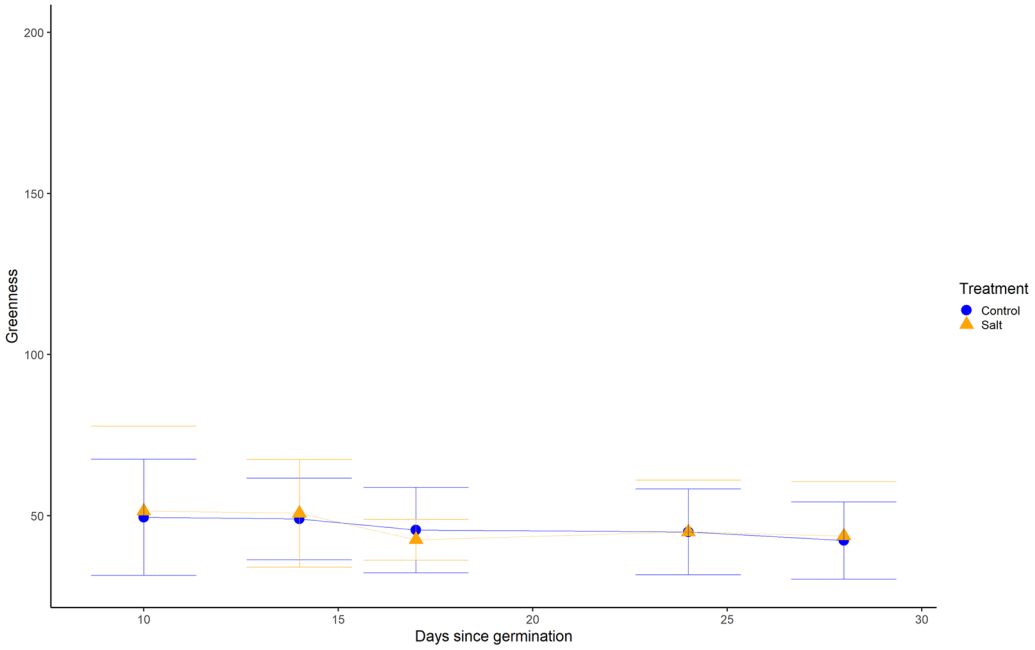


**FIGURE 7** A graph depicting changes in greenness as a function of days since germination for the DSLR images after control and salt treatments. Here, the *y*-axis is truncated to represent the range of possible greenness values after image processing. Each data point represents the mean of between 102 and 141 measurements. Error bars represent the standard deviation of greenness estimates across images from the same day.

manually acquired DSLR images, the HTP system acquired images at a much higher temporal density and reproduced developmental trends and treatment differences for bench-level analyses of foliar area. The HTP system also produced estimates of greenness that were within a comparable range as the estimates acquired from the DSLR images. While there were significant correlations between the two image types in terms of foliar area for both control and salt condition plants, there were no significant correlations between DSLR images and HTP images for measurements

**TABLE 1** Inferential statistics for the linear mixed effects models fit to foliar area and greenness data.

| Dependent variable | Effect | Estimate | SE | df | *t* | *P* |
|---|---|---|---|---|---|---|
| Mean foliar area ($cm^2$) for HTP images | Treatment | 17.931 | 7.526 | 2.125 | 1.689 | 0.227 |
| | Day | 3.988 | 0.043 | 1911.045 | 92.139 | <0.001 |
| | Solar DLI | −0.797 | 0.092 | 1911.098 | −8.673 | <0.001 |
| | Treatment × day | −2.189 | 0.066 | 1911.362 | −33.157 | <0.001 |
| Greenness for HTP images | Treatment | −8.063 | 5.012 | 2.240 | −1.609 | 0.236 |
| | Day | 0.083 | 0.031 | 1911.099 | 2.679 | 0.007 |
| | Solar DLI | 0.245 | 0.066 | 1911.223 | 3.731 | <0.001 |
| | Treatment × day | 0.186 | 0.047 | 1911.794 | 3.937 | <0.001 |
| Foliar area ($cm^2$) for DSLR images | Treatment | 46.620 | 7.611 | 6.498 | 6.125 | <0.001 |
| | Day | 6.512 | 0.0203 | 1242.027 | 32.124 | <0.001 |
| | Treatment × day | −3.802 | 0.287 | 1242.107 | −13.243 | <0.001 |
| Greenness for DSLR images | Treatment | 1.271 | 3.932 | 5.834 | 0.323 | 0.758 |
| | Day | −0.396 | 0.101 | 1242.025 | −3.919 | <0.001 |
| | Treatment × day | −0.051 | 0.143 | 1242.095 | −0.353 | 0.724 |

*Note*: DLI = daily light interval; HTP = high-throughput phenotyping.

of greenness after limiting the analyses to the five days on which DSLR images were collected. Together, these findings highlight the potential of HTP systems built from low-cost hardware and freely available software.

Our inability to detect an effect of the salt treatment on greenness may be attributable to the relatively low concentration of NaCl (54.34 mM) used for the present study. Indeed, previous research on the effect of salt stress on related measurements such as chlorophyll content exposed plants to much higher concentrations of NaCl for a relatively brief period of time (Han et al., 2013; Kim et al., 2016; Navarro-León et al., 2021). For example, Kim et al. (2016) observed interveinal chlorosis and detected significantly lower chlorophyll content in wild-type *B. rapa* after exposure to a 200 mM NaCl solution for one week early in development. For the present study, a lower salt concentration was necessary to allow a majority of the plants to germinate and survive to flowering, but this design makes it impossible to disentangle the effects of salt concentration, duration of exposure, and developmental phase on the greenness detected by the DSLR and HTP camera systems.

The low cost of this HTP system (~US$1000) is important to emphasize because reducing the cost of research on genotype–phenotype relationships with an aim toward crop improvement will help ensure the future of the world's food supply in the long term (Von Braun, 2008; Challinor et al., 2014). The costs of such studies are also often prohibitive for smaller laboratories, smaller farms, and governments with fewer economic resources. Millions of farmers worldwide rely on relatively low-cost crops such as cereals, and advanced high-throughput phenotyping technologies for crop improvement are often prohibitively expensive for these farmers (Prasanna et al., 2013). By reducing these costs, we may help researchers in disadvantaged areas improve crop yield without extremely large investments in technology and expertise.

In addition to its low cost, advantages of this HTP system include that it is easily scalable to larger greenhouses and field studies and is sufficiently flexible to be used for different species, treatments, and developmental time scales. This system is scalable because the images are acquired from each camera sequentially. Unlike HTP systems with conveyors for moving plants toward individual sensors (e.g., Chen et al., 2014; Awlia et al., 2016), the present system employs a larger number of cheap sensors, increasing the temporal density of measurements without adding substantial costs (Yang et al., 2020; Casto et al., 2021). In addition, wireless communication between the Raspberry Pi and the cameras allows the Pi to be stored in a nearby office away from potentially damaging greenhouse conditions (cf. Minervini et al., 2017; Tovar et al., 2018).

Because the analyses of the measurements presented here are relatively simple (i.e., based on RGB images), they can be flexibly applied in a large variety of experimental and applied contexts (e.g., Humplík et al., 2015; Kefauver et al., 2015; An et al., 2016; Ge et al., 2016). In addition, the images captured by the HTP system are high definition, allowing advanced users to apply powerful image analysis

pipelines such as PlantCV (Gehan et al., 2017; Tovar et al., 2018) to address more detailed research or agronomic questions that may be specific to different species or growing conditions (cf. Chen et al., 2014).

One limitation to using a wireless HTP system in the field is the possibility of interference among a large number of GoPro networks, which may be needed to separately monitor individual plants in the field. For example, Mirnezami et al. (2021) mounted approximately 500 cameras to poles next to individual plants to detect anthesis in maize. While the risk of interference may be attenuated by using long-range wide-area network (LoRaWAN) transmission technology for sending and receiving images (Fort et al., 2021), this technology would impose a delay for moderately large data files and is more expensive than GoPro cameras. However, if fewer cameras are sufficient and a researcher is primarily interested in effects spanning blocks of plants, then HTP systems may benefit from placing wireless RGB cameras on poles (Lu et al., 2017) or unmanned aerial vehicles (Liu et al., 2020) to capture overhead images.

Despite the benefits of our simple image analyses using greenness indices, there are some limitations compared to machine learning approaches. First, the system cannot distinguish between plants and objects near the plants that are visibly green. Second, additional layers of classification would need to be included in the image analyses in order to measure individual plant organs such as the size of a specific leaf. Third, for individual plant measurements rather than bench-level estimates, the plants need to be sufficiently spaced out so that there is no overlap in the overhead view of the plants.

Altogether, the HTP system presented in this paper is promising for low-cost and automated data collection at high temporal densities in a large variety of experimental and applied contexts. Future work will focus on validating the use of this system for the measurement of individual genotypes and the study of genotype–phenotype relationships.

## AUTHOR CONTRIBUTIONS

All three authors planned and designed the research. T.T. and H.L. performed the experiment. T.T. analyzed the data and wrote the first draft of the manuscript. T.T. and R.L.B. edited subsequent versions of the manuscript. All authors approved the final version of the manuscript.

## ACKNOWLEDGMENTS

The authors thank Frankie Clark, Abigail Kozyra, and Ryan Gerbitz (Miami University) for their help with watering and plant care during the experiment, as well as the reviewers for their constructive comments and suggestions. Funding for this research was provided by the Department of Biology at Miami University.

## DATA AVAILABILITY STATEMENT

All of the data and analysis scripts have been deposited to Zenodo (data: https://doi.org/10.5281/zenodo.5725224; scripts: https://doi.org/10.5281/zenodo.6366716).

## ORCID

*Tyler Thrash* https://orcid.org/0000-0002-3011-7029
*Robert L. Baker* https://orcid.org/0000-0001-7591-5035

## REFERENCES

Abdallah, S. B., B. Aung, L. Amyot, I. Lalin, M. Lachâal, N. Karray-Bouraoui, and A. Hannoufa. 2016. Salt stress (NaCl) affects plant growth and branch pathways of carotenoid and flavonoid biosynthesis in *Solanum nigrum*. *Acta Physiologiae Plantarum* 38(3): 72.

An, N., C. M. Palmer, R. L. Baker, R. C. Markelz, J. Ta, M. F. Covington, J. N. Maloof, et al. 2016. Plant high-throughput phenotyping using photogrammetry and imaging techniques to measure leaf length and rosette area. *Computers and Electronics in Agriculture* 127: 376–394.

Awlia, M., A. Nigro, J. Fajkus, S. M. Schmoeckel, S. Negrão, D. Santelia, M. Trtilek, et al. 2016. High-throughput non-destructive phenotyping of traits that contribute to salinity tolerance in *Arabidopsis thaliana*. *Frontiers in Plant Science* 7: 1414.

Baker, R. L., W. F. Leong, M. T. Brock, M. J. Rubin, R. C. Markelz, S. Welch, J. N. Maloof, and C. Weinig. 2019. Integrating transcriptomic network reconstruction and eQTL analyses reveals mechanistic connections between genomic architecture and *Brassica rapa* development. *PLoS Genetics* 15(9): e1008367.

Berger, B., B. De Regt, and M. Tester. 2012. High-throughput phenotyping of plant shoots. *In* J. Normanly [ed.], High-throughput phenotyping in plants: Methods and protocols, 9–20. Humana Press, Totowa, New Jersey, USA.

Brien, C. J., B. Berger, H. Rabie, and M. Tester. 2013. Accounting for variation in designing greenhouse experiments with special reference to greenhouses containing plants on conveyor systems. *Plant Methods* 9(1): 5.

Casto, A. L., H. Schuhl, J. C. Tovar, Q. Wang, R. S. Bart, N. Fahlgren, and M. A. Gehan. 2021. Picturing the future of food. *Plant Phenome Journal* 4(1): e20014.

Challinor, A. J., J. Watson, D. B. Lobell, S. M. Howden, D. R. Smith, and N. Chhetri. 2014. A meta-analysis of crop yield under climate change and adaptation. *Nature Climate Change* 4(4): 287–291.

Chen, D., K. Neumann, S. Friedel, B. Kilian, M. Chen, T. Altmann, and C. Klukas. 2014. Dissecting the phenotypic components of crop plant growth and drought responses based on high-throughput image analysis. *Plant Cell* 26(12): 4636–4655.

Fort, A., G. Peruzzi, and A. Pozzebon. 2021. Quasi-real time remote video surveillance unit for LoRaWAN-based image transmission. *In* 2021 IEEE International Workshop on Metrology for Industry 4.0 & IoT (MetroInd4. 0&IoT), 588–593. IEEE, New York, New York, USA.

Ge, Y., G. Bai, V. Stoerger, and J. C. Schnable. 2016. Temporal dynamics of maize plant growth, water use, and leaf water content using automated high throughput RGB and hyperspectral imaging. *Computers and Electronics in Agriculture* 127: 625–632.

Gehan, M. A., N. Fahlgren, A. Abbasi, J. C. Berry, S. T. Callen, L. Chavez, A. N. Doust, et al. 2017. PlantCV v2: Image analysis software for high-throughput plant phenotyping. *PeerJ* 5: e4088.

Giuffrida, M. V., F. Chen, H. Scharr, and S. A. Tsaftaris. 2018. Citizen crowds and experts: Observer variability in image-based plant phenotyping. *Plant Methods* 14(1): 12.

Han, K. H., Y. J. Jung, U. Bayarsaikhan, I. H. Lee, J. S. Choi, I. S. Nou, Y. G. Cho, and K. K. Kang. 2013. Overexpression of BrSAC1 encoding a phosphoinositide phosphatase isolated from Chinese cabbage (*Brassica rapa* L.) improved tolerance to cold, dehydration, and salt stresses in transgenic tobacco. *African Journal of Biotechnology* 12(15): 1782–1792.

Hasanuzzaman, M., L. Shabala, M. Zhou, T. J. Brodribb, R. Corkrey, and S. Shabala. 2018. Factors determining stomatal and non-stomatal (residual) transpiration and their contribution towards salinity tolerance in contrasting barley genotypes. *Environmental and Experimental Botany* 153: 10–20.

Humplík, J. F., D. Lazár, T. Fürst, A. Husičková, M. Hýbl, and L. Spíchal. 2015. Automated integrative high-throughput phenotyping of plant

shoots: A case study of the cold-tolerance of pea (*Pisum sativum* L.). *Plant Methods* 11(1): 20.

Kefauver, S. C., G. El-Haddad, O. Vergara-Diaz, and J. L. Araus. 2015. RGB picture vegetation indexes for high-throughput phenotyping platforms (HTPPs). *In* C. M. U. Neale and A. Maltese [eds.], Remote sensing for agriculture, ecosystems, and hydrology XVII, Vol. 9637, p. 96370 J. International Society for Optics and Photonics, Bellingham, Washington, USA.

Kim, J. A., H. E. Jung, J. K. Hong, V. Hermand, C. Robertson McClung, Y. H. Lee, J. Y. Kim, et al. 2016. Reduction of *GIGANTEA* expression in transgenic *Brassica rapa* enhances salt tolerance. *Plant Cell Reports* 35(9): 1943–1954.

Li, L., Q. Zhang, and D. Huang. 2014. A review of imaging techniques for plant phenotyping. *Sensors* 14(11): 20078–20111.

Liu, Y., C. Cen, Y. Che, R. Ke, Y. Ma, and Y. Ma. 2020. Detection of maize tassels from UAV RGB imagery with faster R-CNN. *Remote Sensing* 12(2): 338.

Lu, H., Z. Cao, Y. Xiao, B. Zhuang, and C. Shen. 2017. TasselNet: Counting maize tassels in the wild via local counts regression network. *Plant Methods* 13(1): 79.

Minervini, M., M. V. Giuffrida, P. Perata, and S. A. Tsaftaris. 2017. Phenotiki: An open software and hardware platform for affordable and easy image-based phenotyping of rosette-shaped plants. *Plant Journal* 90(1): 204–216.

Mirnezami, S. V., S. Srinivasan, Y. Zhou, P. S. Schnable, and B. Ganapathysubramanian. 2021. Detection of the progression of anthesis in field-grown maize tassels: A case study. *Plant Phenomics* 2021: 4238701.

Navarro-León, E., V. Paradisone, F. J. López-Moreno, J. J. Rios, S. Esposito, and B. Blasco. 2021. Effect of CAX1a TILLING mutations on photosynthesis performance in salt-stressed *Brassica rapa* plants. *Plant Science* 311: 111013.

Prasanna, B. M., J. L. Araus, J. Crossa, J. E. Cairns, N. Palacios, B. Das, and C. Magorokosho. 2013. High-throughput and precision phenotyping for cereal breeding programs. *In* P. K. Gupta and R. K. Varshney [eds.], Cereal genomics II, p. 341–374. Springer, Dordrecht, the Netherlands.

Ray, D. K., N. D. Mueller, P. C. West, and J. A. Foley. 2013. Yield trends are insufficient to double global crop production by 2050. *PLoS ONE* 8(6): e66428.

Richardson, A. D., J. P. Jenkins, B. H. Braswell, D. Y. Hollinger, S. V. Ollinger, and M. L. Smith. 2007. Use of digital webcam images to track spring green-up in a deciduous broadleaf forest. *Oecologia* 152(2): 323–334.

Tovar, J. C., J. S. Hoyer, A. Lin, A. Tielking, S. T. Callen, S. Elizabeth Castillo, M. Miller, et al. 2018. Raspberry Pi–powered imaging for plant phenotyping. *Applications in Plant Sciences* 6(3): e1031.

Toxopeus, H., H. Yamagishi, and E. H. Oost. 1987. A cultivar group classification of *Brassica rapa* L., update 1987. *Cruciferae Newsletter* 12: 5–6.

Von Braun, J. 2008. The food crisis isn't over. *Nature* 456(7223): 701.

Yang, W., H. Feng, X. Zhang, J. Zhang, J. H. Doonan, W. D. Batchelor, L. Xiong, and J. Yan. 2020. Crop phenomics and high-throughput phenotyping: Past decades, current challenges, and future perspectives. *Molecular Plant* 13(2): 187–214.

## SUPPORTING INFORMATION

Additional supporting information can be found online in the Supporting Information section at the end of this article.

**Appendix S1**. The exact models in R notation that were used for analyzing the interaction between condition and day on foliar area and greenness for both HTP and DSLR images.

**How to cite this article:** Thrash, T., H. Lee, and R. L. Baker. 2022. A low-cost high-throughput phenotyping system for automatically quantifying foliar area and greenness. *Applications in Plant Sciences* 10(6): e11502. https://doi.org/10.1002/aps3.11502